CrossMark

DISCOVERY OF A MILLISECOND PULSAR IN THE 5.4 DAY BINARY 3FGL J1417.5–4402: OBSERVING THE LATE PHASE OF PULSAR RECYCLING

F. Camilo[1,2], J. E. Reynolds[3], S. M. Ransom[4], J. P. Halpern[1], S. Bogdanov[1], M. Kerr[3], P. S. Ray[5], J. M. Cordes[6], J. Sarkissian[7], E. D. Barr[8], and E. C. Ferrara[9]

[1] Columbia Astrophysics Laboratory, Columbia University, New York, NY 10027, USA
[2] SKA South Africa, Pinelands, 7405, South Africa
[3] CSIRO Astronomy and Space Science, Australia Telescope National Facility, Epping, NSW 1710, Australia
[4] National Radio Astronomy Observatory, Charlottesville, VA 22903, USA
[5] Space Science Division, Naval Research Laboratory, Washington, DC 20375-5352, USA
[6] Department of Astronomy and Center for Radiophysics and Space Research, Cornell University, Ithaca, NY 14853, USA
[7] CSIRO Parkes Observatory, Parkes, NSW 2870, Australia
[8] Centre for Astrophysics and Supercomputing, Swinburne University of Technology, Hawthorn, VIC 3122, Australia
[9] NASA Goddard Space Flight Center, Greenbelt, MD 20771, USA

ABSTRACT

In a search of the unidentified *Fermi* gamma-ray source 3FGL J1417.5–4402 with the Parkes radio telescope, we discovered PSR J1417–4402, a 2.66 ms pulsar having the same 5.4 day orbital period as the optical and X-ray binary identified by Strader et al. The existence of radio pulsations implies that the neutron star is currently not accreting. Substantial outflows from the companion render the radio pulsar undetectable for more than half of the orbit, and may contribute to the observed Hα emission. Our initial pulsar observations, together with the optically inferred orbit and inclination, imply a mass ratio of 0.171 ± 0.002, a companion mass of $M_2 = 0.33 \pm 0.03\,M_\odot$, and a neutron star mass in the range $1.77 \leqslant M_1 \leqslant 2.13\,M_\odot$. However, there remains a discrepancy between the distance of 4.4 kpc inferred from the optical properties of the companion and the smaller radio dispersion measure distance of 1.6 kpc. The smaller distance would reduce the inferred Roche-lobe filling factor, increase the inferred inclination angle, and decrease the masses. As a wide binary, PSR J1417–4402 differs from the radio-eclipsing black widow and redback pulsars being discovered in large numbers by *Fermi*. It is probably a system that began mass transfer onto the neutron star after the companion star left the main sequence. The companion should end its evolution as a He white dwarf in a 6–20 day orbit, i.e., as a typical binary millisecond pulsar companion.

Key words: pulsars: individual (PSR J1417–4402)

1. INTRODUCTION

The Large Area Telescope (LAT; Atwood et al. 2009) on the *Fermi Gamma-ray Space Telescope* has been used to detect 200 rotation-powered pulsars (e.g., Abdo et al. 2013).[10] Nearly half of them are millisecond pulsars (MSPs; e.g., Abdo et al. 2009). Half of the LAT-detected MSPs were discovered prior to *Fermi* in "all-sky" radio surveys. The other half were discovered in directed radio searches of LAT unidentified sources (e.g., Ray et al. 2012).

These two subpopulations differ in at least one important respect: 95% of the MSPs discovered in all-sky surveys have white dwarf companions or are isolated. By contrast, 40% of those discovered in LAT-guided searches are in compact (<1 day) interacting binaries—the so-called "black widow" or "redback" systems. Black widow pulsars have degenerate $\approx 0.03\,M_\odot$ companions and many are regularly eclipsed at radio wavelengths near pulsar superior conjunction. Redback MSPs have hot and bloated main sequence-like $\gtrsim 0.1\,M_\odot$ companions and display irregular radio eclipses that can persist for more than half of the orbit.

Black widows have long been considered to possibly represent the final stage in the creation of isolated MSPs, but many uncertainties remain (e.g., Podsiadlowski et al. 2002). How redbacks fit into the recycling scenario of MSP formation, and how they may relate to black widows, is even more uncertain

(e.g., Chen et al. 2013; Benvenuto et al. 2014). No redbacks were known in the Galactic disk prior to *Fermi*, and they continue to present unexpected behavior: e.g., three redbacks have transitioned rapidly between accretion-disk states with no radio pulsations and rotation-powered states with radio pulsations (Archibald et al. 2009; Papitto et al. 2012; Stappers et al. 2014).

In this context, Strader et al. (2015) have discovered a peculiar system. They report on multi-wavelength observations of the unidentified source now known as 3FGL J1417.5–4402, finding a variable X-ray object associated with an optical counterpart that displays ellipsoidal variations with a $P_b = 5.4$ day binary period. They interpret the observation of double-peaked Hα emission as evidence for an accretion disk in a low-mass X-ray binary, and conclude that the optical/IR star is a $\approx 0.35\,M_\odot$ giant at a distance of 4.4 kpc and that the neutron star is massive, $\approx 2.0\,M_\odot$. Strader et al. (2015) proposed that 3FGL J1417.5–4402 could be a transitioning MSP that might eventually be detectable as a radio pulsar. However, the large orbit sets PSR J1417–4402 apart from Galactic redbacks: all those previously known have $P_b < 1$ day.

Here we report the discovery and initial study of a radio MSP that is clearly the neutron star in the 5.4 day binary 3FGL J1417.5–4402. Although it shares some of the properties of redbacks, such as their companion masses and extensive radio eclipses, PSR J1417–4402 is on a standard evolutionary track that will end as a typical binary MSP with a low-mass white dwarf companion, as Strader et al. (2015) deduced. It is the first such system to be identified in the Galaxy.

---

[10] https://confluence.slac.stanford.edu/display/GLAMCOG/Public+List+of+LAT-Detected+Gamma-Ray+Pulsars

Table 1
New Radio Searches of 3FGL Sources at Parkes

Source Name[a]	Integration Time (minutes)	N_{obs}[b]
3FGL J0940.6−7609	60, 60, 60, 41	5
3FGL J1025.1−6507	60, 60, 60, 45	5
3FGL J1231.6−5113	60, 80, 98, 52	5
3FGL J1325.2−5411	60	2
3FGL J1417.5−4402	60	2
3FGL J1753.6−4447	60	2
3FGL J1803.3−6706	55	2
3FGL J1831.6−6503	60	2
3FGL J2043.8−4801	45	3
3FGL J2131.1−6625	60, 60, 60	5
3FGL J2200.0−6930	55, 60, 60	4
3FGL J2333.0−5525	60, 60, 60, 38	6

Notes.
[a] Source properties, including the positions that we targeted in our searches, are given in Acero et al. (2015). See also Camilo et al. (2015).
[b] Number of radio searches done, including those listed here and in Camilo et al. (2015).

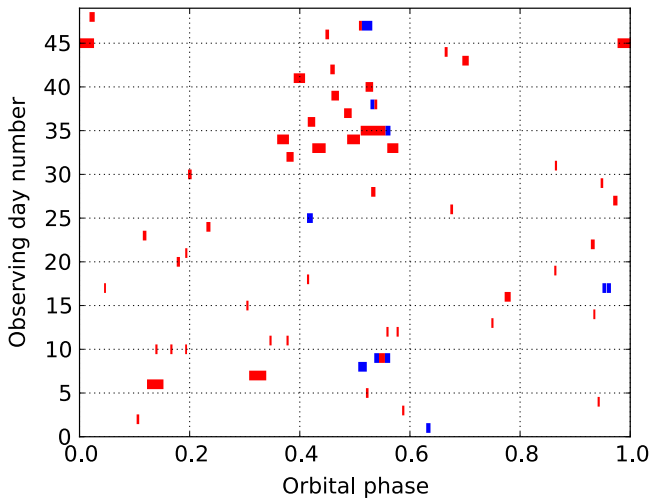## 2. OBSERVATIONS

2.1. Radio Searches at Parkes

In Camilo et al. (2015) we reported on a radio survey of 56 unidentified LAT sources using the CSIRO Parkes telescope. We discovered 10 MSPs, in some cases only after multiple observations of each source. Multiple observations increase the chance that an otherwise detectable pulsar will not be missed due to interstellar scintillation, large acceleration at a particularly unfavorable binary phase, or eclipse. We established that 23 of the remaining unidentified sources had gamma-ray properties consistent with those of known pulsars, and therefore were deserving of further radio searches.

During 2015 March–May we performed 28 search observations of 12 of the highest-ranked LAT targets remaining from our original source list (Table 1). Because the analog filterbank used in the original survey had in the meantime been decommissioned, we used instead a digital filterbank (PDFB4, see Manchester et al. 2013) to record data from the central beam of the Parkes 20 cm multibeam receiver, at a center frequency of 1369 MHz. Each of 512 0.5 MHz wide polarization-summed channels was sampled with PDFB4 every 80 μs for approximately 1 hr (see Table 1), and the resulting power measures were written with 2 bit precision to disk for off-line analysis.

We analyzed the data using PRESTO (Ransom 2001), exactly as for our earlier searches described in Camilo et al. (2015). In an observation of 3FGL J1417.5–4402 done on 2015 March 28, we discovered a binary pulsar with period $P = 2.66$ ms and dispersion measure DM $= 55$ pc cm^{-3} (Figure 1(a)). To our knowledge, this is the first pulsar discovered using any of the PDFBs. We then realized that 3FGL J1417.5–4402 was the gamma-ray source in which Strader et al. (2015) had discovered an unusual binary, and sought to determine whether the new pulsar was related.
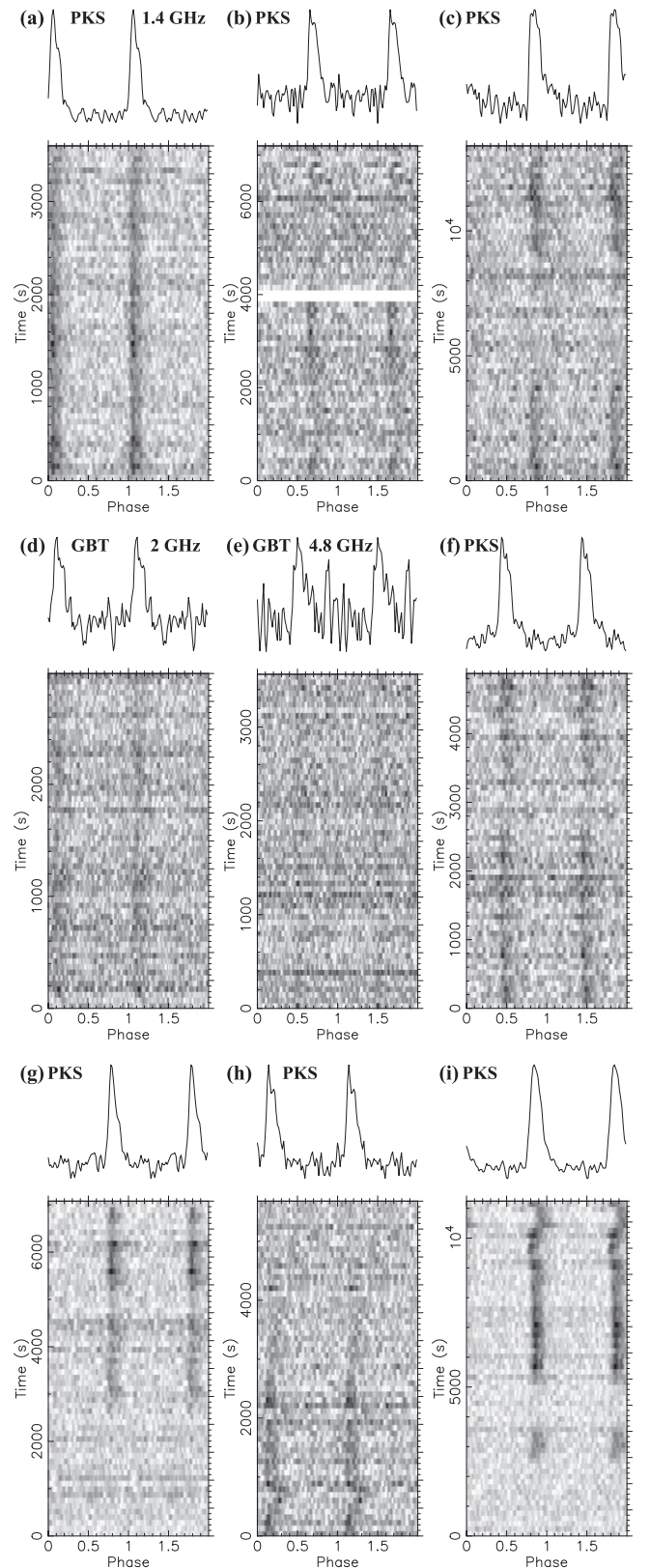
Figure 1. All radio detections of PSR J1417–4402 reported in this paper, in time order (see also Figure 2). All Parkes detections are at 1.4 GHz. Individual integration times range between 1 and 4 hr. The folded pulse profiles are shown twice as a function of time and summed at the top.

Figure 2. Fifty six observations of PSR J1417–4402 on 48 days during 2015 March–2016 January as a function of orbital phase ϕ_b. Non-detections are represented in red, blue indicates detections. The detection at $\phi_b \approx 0.95$ represents two adjoining GBT observations, at 2 GHz and 5 GHz respectively (see Figures 1(d)–(e)). The non-detections on day numbers 16 and 20 are at 2 GHz; all other observations are from Parkes at 1.4 GHz.

Table 2
Parameters of PSR J1417–4402

Parameter	Value
Timing Parameters	
Right ascension, R.A. (J2000.0)[a]	$14^h 17^m 30^s.604$
Declination, decl. (J2000.0)[a]	$-44°02'57''.37$
Spin period, P (ms)	2.6642160(4)
Dispersion measure, DM (pc cm^{-3})	55.00(3)
Binary period, P_b (d)	5.37372(3)
Projected semimajor axis, x_1 (l-s)	4.876(9)
Time of ascending node, T_{asc} (MJD)	57111.457(2)
Derived Parameters	
Galactic longitude, l	318°.86
Galactic latitude, b	16°.14
DM-derived distance, d (kpc)[b]	1.6
Pulsar mass function, f_1 ($M_\odot$)	0.00433

Notes. Numbers in parentheses represent uncertainties on the last digit. See Section 2.2 for a description of the fits.
[a] Fixed at the optical position (Strader et al. 2015).
[b] From the electron density model of Cordes & Lazio (2002) (see Section 3.1).

2.2. Timing Observations of PSR J1417–4402

We had searched the location of the new pulsar once before (Table 1), unsuccessfully. Following its discovery we began Parkes timing observations at 1.4 GHz. Between 2015 March 28 and 2016 January 14 we have observed PSR J1417–4402 52 times on 46 days for a total of 75 hr, and have detected it for a total of 11 hr on seven days (Figures 1(a)–(c) and (f)–(i)). All of these detections were within orbital phases $0.4 < \phi_b < 0.65$, which we have observed for 42 hr (see Figure 2; throughout this paper we use the radio phase convention, in which $\phi_b = 0$ is the time of ascending node of the pulsar). Two thirds of these observing sessions, 85% of the observing time, and all of the detections, used the same PDFB4 setup employed in the discovery observation. The remaining timing observations were done with the Berkeley-Parkes-Swinburne Recorder (BPSR), which in effect samples 340 MHz of bandwidth centered on 1352 MHz every 64 μs with 0.4 MHz resolution (for more details, see Keith et al. 2010).

For the relatively large DM of PSR J1417–4402 we do not expect interstellar scintillation to modulate the detected flux density by more than a factor of ~2. Some, likely all, of the non-detections are caused by eclipses, as in Figure 1 (panels (c), (g)–(i)). On at least two occasions (see "kinks" lasting for ≈ 500 s near the beginning/end of the observations in Figure 1(h)/(i)) the pulse arrival is delayed by $\approx 0.15 P$, presumably due to an ephemeral clump of ionized material. This time delay corresponds to an extra electron column δDM ≈ 0.15 pc cm^{-3}.

In 2015 June we observed PSR J1417–4402 at the Robert C. Byrd Green Bank Telescope (GBT). We did this on three days for a total of 3 hr at a central frequency of 2 GHz, recording a bandwidth of 800 MHz using GUPPI.[11] One of these observations resulted in a detection (Figure 1(d)), at $\phi_b \approx 0.95$ (Figure 2). On the same day we also did a 1 hr observation using the new GBT C-band receiver, centered at 4.8 GHz with 800 MHz bandwidth, and detected the pulsar with an estimated flux density of ≈ 40 μJy (Figure 1(e)).

Additionally, we observed PSR J1417–4402 during 2015 April–June at Parkes at 0.7 GHz (once for 0.6 hr) and 3.1 GHz (twice for a total of 1.3 hr), and at the GBT at 350 MHz (three times, 0.6 hr). Finally, in a different Parkes survey of *Fermi* unidentified sources, we had also observed its location at 1.4 GHz in 2014 July (three times, 2.1 hr). None of these observations resulted in detections.

There are currently too few radio detections to obtain a phase-connected timing solution. However, the existing detections (all of which indicated orbital acceleration) were sufficient to determine that PSR J1417–4402 is the neutron star in the Strader et al. (2015) binary: it has the same orbital period and its phase is 180° shifted from that of the optical star. In order to obtain the parameters listed in Table 2 we first extracted pulse times of arrival (TOAs) from all detections. Using the TEMPO[12] timing software we fit each day's TOAs to a model including spin frequency and up to two derivatives as needed. We then did a least-squares fit of a circular orbit ($e < 0.02$ according to Strader et al. 2015) to the resulting overall set of Doppler-shifted barycentric spin frequencies. We also used TEMPO to directly fit a zero-eccentricity binary model to the TOAs, allowing for an arbitrary offset between daily sets of TOAs (i.e., the resulting solution is not phase connected). The parameters and uncertainties given in Table 2 encompass the sets of values returned by these two independent fits. Our scant detections currently span a narrow range of binary phases (Figure 2), and we expect greatly improved orbital parameters as detections accumulate; nevertheless, our values for P_b and T_{asc} already have 10 times the precision of those obtained from optical observations.

2.3. X-Ray and UV Observations of PSR J1417–4402

The *Swift* X-ray Telescope (XRT, Burrows et al. 2005) observed PSR J1417–4402 in 2015 March and June, for a total of 12.5 ks. The eight observations in March spanned slightly more than one binary orbit (Table 3). We processed all *Swift*

---

[11] https://safe.nrao.edu/wiki/bin/view/CICADA/GUPPiUsersGuide

[12] http://tempo.sourceforge.net

Table 3
Swift XRT and UVOT Observations of PSR J1417−4402

ObsID	Date (UT)	Exposure Time (ks)	Binary Phase[a] (ϕ_b)	XRT Count Rate (0.3–10 keV) (10^{-2} s^{-1})	UVOT Filter	Magnitude[b]
00084749001	2015 Mar 13	0.4	0.89	$1.8^{+0.9}_{-0.7}$	$uvm2$	>18.60
00084749002	2015 Mar 14	1.8	0.94	$1.2^{+0.4}_{-0.3}$	$uvw1$	$18.98 \pm 0.11 \pm 0.03$
00084749004	2015 Mar 15	1.6	0.33	1.1 ± 0.3	u	$18.22 \pm 0.05 \pm 0.02$
00084749005	2015 Mar 16	1.8	0.41	2.35 ± 0.45	$uvw2$	>20.26
00084749006	2015 Mar 17	0.5	0.55	4.0 ± 1.0	$uvm2$	>19.93
00084749007	2015 Mar 18	1.4	0.78	$0.8^{+0.4}_{-0.3}$	$uvw1$	>18.22
00084749008	2015 Mar 19	1.4	0.95	1.3 ± 0.4	u	$17.85 \pm 0.04 \pm 0.02$
00084749009	2015 Mar 20	1.7	0.09	1.8 ± 0.4	$uvw2$	>19.84
00084749010	2015 Jun 18	2.1	0.82	1.7 ± 0.3	$uvw1$	$19.28 \pm 0.13 \pm 0.03$

Notes. All uncertainties represent 90% confidence levels.
[a] Phase 0.75 corresponds to companion superior conjunction. These ϕ_b values are based on the radio ephemeris of Table 2.
[b] For measured magnitudes (in the Vega system, Breeveld et al. 2011), the first uncertainty is statistical and the second is systematic.

observations using FTOOLS version 6.16.[13] The 0.3–10 keV spectrum and light curve from the XRT photon counting mode data were obtained with XSELECT. The source events were extracted from a circular aperture of radius 20 pixels (47″), while the background was taken from an annulus with an inner radius of 60 pixels and an outer radius of 110 pixels.

The X-ray count rates appear to show variability, with a maximum at binary phase $\phi_b = 0.55$. However, the probability that the observed counts arise from a constant flux distribution is 2.4% (determined from a χ^2 fit of a model with a constant count rate to the X-ray light curve), so we cannot rule out the null hypothesis that the flux is constant. The combined time-averaged X-ray spectrum is well-fitted using XSPEC by an absorbed power-law with photon index $\Gamma = 1.59^{+0.35}_{-0.20}$, column density $N_{\rm H} = 2.2^{+1.7}_{-1.3} \times 10^{21}$ cm^{-2}, and an unabsorbed 0.3–10 keV flux of $(8.7 \pm 1.5) \times 10^{-13}$ erg cm^{-2} s^{-1} (all uncertainties in this section represent 90% confidence levels). This is consistent with the spectrum measured from a 2011 *Chandra* observation (Strader et al. 2015), and corresponds to an X-ray luminosity of $\approx 3 \times 10^{32}$ $(d/1.6$ kpc$)^2$ erg s^{-1}, which we scale according to the DM-derived distance (see Section 3.1 for a discussion of this).

Simultaneously with the XRT, PSR J1417−4402 was observed with the *Swift* ultraviolet and optical telescope (UVOT, Roming et al. 2005), through a variety of filters. The resulting magnitudes and upper limits are also presented in Table 3. The UVOT photometric measurements were obtained using the uvotsource command in FTOOLS. The source flux was obtained from a 5″ circle, while the background was taken from a source-free circular region of radius 20″. There are two detections in u and two in $uvw1$. The remaining UV observations yield only upper limits. The implications of these will be discussed in Section 3.2.

3. DISCUSSION

3.1. What is the Distance to PSR J1417−4402?

Strader et al. (2015) estimate that the PSR J1417−4402 system lies at a distance of $d = 4.4$ kpc (with a likely uncertainty of at least 20%) based on the magnitude and optical spectrum of the companion, and assuming that it fills its Roche lobe. Given the poor pulsar detectability (generally low signal-to-noise ratio and frequent eclipses), it is unlikely that a parallax will be measured

either interferometrically or through timing observations. But we can estimate the distance from the radio pulsar DM. The Cordes & Lazio (2002) electron distribution model (NE2001) gives $d_{\rm NE2001} = 1.6$ kpc, while the previously most used electron density model gives $d_{\rm TC93} = 3.0$ kpc (Taylor & Cordes 1993).

We favor the NE2001 distance because TC93 generally over-predicts distances and fails to account for the DMs of about 10% of pulsars (Cordes & Lazio 2002, and unpublished reanalysis of the ATNF pulsar catalog). Of 66 pulsars with parallax measurements[14], 17 have DMs between 35 and 75 pc cm^{-3} (compared to 55 pc cm^{-3} for PSR J1417−4402). Of these, 10 have NE2001-estimated distances that are consistent to within 20% of the parallax distance ranges (only one of the 10 had a well constrained distance used to construct NE2001). The remaining seven objects have distances that disagree by more than 20%, in some cases by a factor of 2. Four have NE2001 distances larger than the parallax distances and the opposite is the case for the other three pulsars.

We conclude that there is no identifiable distance bias in NE2001 (as there is for TC93) and that the NE2001 distance is the best provisional DM-based distance estimate. However, due to possible variations in the scale height of the electron density distribution, there is considerable uncertainty in determining DM distances to pulsars at high Galactic latitude when DM sin|b| is comparable to its maximum value (see Figure 1 of Cordes & Lazio 2003). PSR J1417−4402 falls in this uncertain regime. Also, a recent study reports new MSP parallax distances that in some cases differ from the NE2001 distances by a factor of 2 (Matthews et al. 2016). Therefore, we do not exclude a larger distance such as that derived by Strader et al. (2015). The conflict between these independent distance measurements, 4.4 and 1.6 kpc, extends to the assumptions made by Strader et al. (2015) in modeling the inclination angle of the system and the masses, because the star would only fill a fraction of the Roche lobe if at the smaller DM-based distance. These issues are discussed in Section 3.3.

3.2. Is There an Accretion Disk?

Strader et al. (2015) concluded that an accretion disk is present, primarily because of the double-peaked Hα emission line, but also because the X-ray luminosity at their preferred distance of 4.4 kpc is consistent with those of transitional MSPs

---

in their disk states. The detection of radio pulsations from PSR J1417–4402 brings that interpretation into question because the transitional MSPs PSR J1023+0038 (Bogdanov et al. 2015) and XSS J12270−4859 (Hill et al. 2011) show no evidence for radio pulsations in their accreting states. Along with the detection of accretion-powered X-ray pulsations in both systems (Archibald et al. 2015; Papitto et al. 2015), this is an indication that the radio pulsar mechanism of these two MSPs is completely quenched by the accretion flow (see also Cordes & Shannon 2008, and references therein).

If the lower DM distance is adopted, the X-ray luminosity of $\approx 3 \times 10^{32} (d/1.6\,\mathrm{kpc})^2$ erg s^{-1} (Section 2.3) is comparable to $\sim 10^{32}$ erg s^{-1} measured for the nearby redback PSR J1723 −2837 (Bogdanov et al. 2014) and lower than the average accreting luminosity of the transitional MSPs (e.g., Linares 2014). Non-thermal X-rays typically observed in redbacks seems to originate from an intra-binary shock driven by the interaction of the pulsar wind and matter from the companion (Arons & Tavani 1993). However, the uncertain distance to PSR J1417–4402 (Section 3.1) and possible X-ray variability (Strader et al. 2015 and Section 2.3) make existing X-ray observations an unreliable discriminator for the presence or absence of accretion.

Even if no accretion flow is reaching the neutron star and the X-rays are not accretion powered, a disk that is truncated at the magnetospheric radius or beyond could still radiate in the ultraviolet and visible. However, the optical and UV continuum data disfavor an accretion disk. While Strader et al. (2015) measured a V_0 magnitude (corrected for extinction) spanning 15.64–15.91, PSR J1417–4402 is much fainter in u and especially in the UV filters (Table 3). Correcting the *Swift u* magnitudes for an extinction $A_u = 0.50$ (Schlafly & Finkbeiner 2011), we find $u_0 = 17.35$ and 17.72 at $\phi_b = 0.95$ and 0.33, respectively. Then $1.7 \leqslant u_0 - V_0 \leqslant 1.9$, which is in the correct range for giant stars of spectral type G8–K0, which have $1.5 \leqslant U_0 - V_0 \leqslant 1.9$ (Pickles 1998). This is the type inferred by Strader et al. (2015) from the optical spectrum of the companion. Thus, there is no evidence for extra light in the ultraviolet coming from an accretion disk. Also, the ultraviolet flux detections, being higher at $\phi_b = 0.95$ than at $\phi_b = 0.33$, and faintest at $\phi_b = 0.82$, are consistent in magnitude and phase with the observed modulation due to ellipsoidal variations that dominate the optical light curves in Strader et al. (2015).

However, since the companion star is likely a giant or subgiant (see below), it is brighter than the redback companions and could mask an accretion-disk component. We can estimate an upper limit on a mass-transfer rate under the conservative assumption that <50% of the minimum observed u-band flux is contributed by a standard blackbody disk (Frank et al. 2002) that is truncated at the pulsar corotation radius, $r_{\mathrm{co}} = 36$ km for a 2 $M_\odot$ neutron star. For an inclination angle of 58° (see Section 3.3) and a distance of 1.6 kpc, the limit is $\dot{m} < 4 \times 10^{14}$ g s^{-1}. The u-band luminosity of a disk is barely changed even if it is truncated at the light cylinder radius, $r_{\mathrm{lc}} = 127$ km for PSR J1417–4402.

This can be compared with $\dot{m} \approx 1 \times 10^{15}$ g s^{-1} estimated by Papitto & Torres (2015) for the demonstrably accreting transitional objects PSR J1023+0038 and XSS J12270−4859 using similar assumptions. And if the distance to PSR J1417–4402 is actually 4.4 kpc, then it could have a similar accretion rate as the transitional pulsars. Note that, in all of these cases, a disk with such a low accretion rate cannot actually reach

the corotation radius, and most of the matter is propelled away (Papitto & Torres 2015). This leaves the possibility that the Hα could be emitted either from the outer disk or in a wind.

The current properties of PSR J1417–4402 appear to be most reminiscent of the eclipsing radio MSP J1740−5340 in the globular cluster NGC 6397 (D'Amico et al. 2001), which is bound to a "red straggler"/sub-subgiant companion in a 1.3 day orbit. However this system was likely formed in an exchange interaction in the dense cluster environment (Orosz & van Kerkwijk 2003), with an evolutionary path substantially different from that of PSR J1417–4402. The bolometric luminosity of the PSR J1417–4402 companion, determined by Strader et al. (2015) for a distance of 4.4 kpc, is reduced by a factor of 7.6 at the DM-derived 1.6 kpc, making it comparable to that of subgiants. PSR J1740−5340 exhibits radio eclipses around superior conjunction for 40% of the orbit, as well as random DM variations at all phases. Its X-ray spectrum is non-thermal (with $\Gamma = 1.7$) and possibly modulated at the binary period (Bogdanov et al. 2010), suggestive of an intra-binary shock. Perhaps most importantly, PSR J1740 −5340 also exhibits a prominent Hα emission line with complex morphology and strong orbital phase dependence (Sabbi et al. 2003), which can be interpreted as being produced in part by a wind from the secondary star that is driven out of the binary by the pulsar wind. The clear evidence for an active rotation-powered radio pulsar suggests that PSR J1417–4402 is presently in the so-called "radio ejection" regime (Ruderman et al. 1989; Burderi et al. 2002) in which any Roche lobe overflow through the L1 point cannot overcome the barrier imposed by the pulsar wind pressure. A larger orbit actually favors this scenario according to Burderi et al. (2002).

One might also consider the possibility that the system transitions rapidly between accreting and non-accreting states. But Hα emission, as evidence for accretion, was detected by Strader et al. (2015) in more than one dozen observations spanning 1 year through 2015 February, while the first detection of radio pulsations, ruling out accretion onto the neutron star, occurred only one month later (Section 2.1). Given all the available evidence, we favor an interpretation in which the PSR J1417–4402 system was not accreting at the time of the optical and radio observations.

3.3. Component Masses

If the mass ratio and the inclination angle of the system can be determined with precision, then the mass of the neutron star can also be measured. This is of particular interest because Strader et al. (2015) concluded that the neutron star is massive, $M_1 = 1.97 \pm 0.15\,M_\odot$. Assuming a tidally locked, Roche-lobe filling secondary, they obtained a mass ratio $q \equiv M_2/M_1 = 0.18 \pm 0.01$ from a measurement of the projected rotational velocity of the secondary (which has unspecified systematic uncertainties) and its radial velocity semi-amplitude $K_2 = 115.7 \pm 1.1$ km s^{-1}. They also assumed a Roche-lobe filling star to fit the optical light curves for the orbital inclination angle using an ellipsoidal model, finding $i = 58° \pm 2°$.

Using the pulsar projected semimajor axis x_1 (Table 2) we infer that the pulsar radial velocity semi-amplitude is 19.8 km s^{-1}. Along with K_2 this implies $q = 0.171 \pm 0.002$, limited by the precision on K_2. Figure 3 shows the masses of the neutron star and companion as a function of inclination angle, allowing for the uncertainties on K_2 and x_1. For $56° \leqslant i \leqslant 60°$, M_1 ranges over 1.77–2.13 $M_\odot$, and
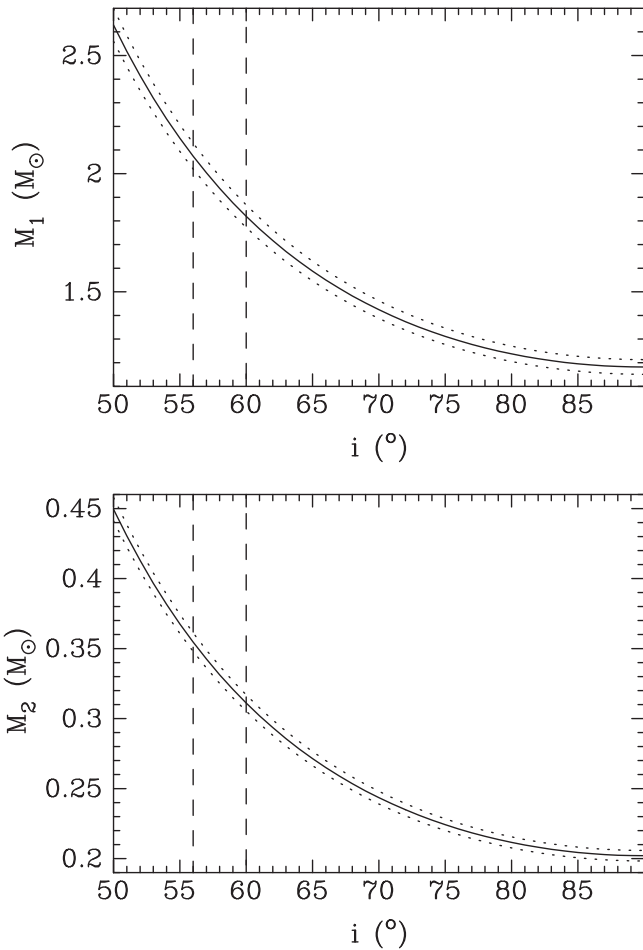
Figure 3. Masses of the neutron star (top) and companion (bottom) as a function of inclination angle i. The dotted curves allow for the uncertainties in the measured orbital velocities of the two stars, as quoted in the text. Strader et al. (2015) modeled i as $58° \pm 2°$ (vertical dashed lines). But i should be larger if the companion is not filling its Roche lobe.

$M_2 = 0.33 \pm 0.03\,M_\odot$. However, if located at the smaller DM-based distance, the radius of the companion is only 0.36 times the Roche-lobe radius; its tidal distortion is reduced, and a larger i would be necessary to fit the ellipsoidal modulation, resulting in smaller masses. The minimum allowed masses (for $i = 90°$) are $M_2 \geqslant 0.20\,M_\odot$ and $M_1 \geqslant 1.15\,M_\odot$. The Roche lobe radius decreases only slightly, from $4.1\,R_\odot$ at $i = 58°$ to $3.5\,R_\odot$ at $i = 90°$ according to the formula of Eggleton (1983), so a higher inclination at the smaller distance would not allow the companion to contact the Roche lobe.

3.4. No Photospheric Heating

The optical light curves (Strader et al. 2015), dominated as they are by ellipsoidal modulation, show no evidence for heating of the companion's photosphere by the pulsar wind. This is probably because the intrinsic luminosity of the giant/subgiant dominates. We can place an upper limit on the spin-down luminosity $\dot{E}$ of the pulsar, or more precisely, on the product of $\dot{E}$ and an efficiency factor η that includes the physics of reprocessing and any anisotropy of the pulsar wind. A heating effect can be approximated using $\eta \dot{E} R_2^2 / 4a^2 = 2\pi R_2^2 \sigma (T_h^4 - T_{\rm eff}^4)$, where $T_{\rm eff}$ is the intrinsic temperature of the unheated star, T_h is the average temperature

of the side facing the pulsar, R_2 is the radius of the companion, and a is the orbital separation.

We use $T_{\rm eff} = 5000$ K from the optical spectrum of Strader et al. (2015), and assume an upper limit of 5200 K for T_h based on the absence of a heating signature at the level of 0.1–0.2 magnitudes. For $i = 58°$, the orbital separation is $a = 17\,R_\odot$, and the limit on $\eta\dot{E}$ is 2.1×10^{35} erg s^{-1}. If instead we assume as a maximum $i = 72°$ (for which $M_1 = 1.4\,M_\odot$), then $a = 15.2\,R_\odot$ and $\eta\dot{E} < 1.7 \times 10^{35}$ erg s^{-1}. Neither of these limits are very restrictive, as η is likely to be less than unity. These limits can also accommodate the gamma-ray luminosity of 3FGL J1417.5–4402, 3×10^{34} erg s^{-1} at a distance of 4.4 kpc (see Section 4).

3.5. Evolutionary Track

With a binary period of 5.4 days, PSR J1417–4402 is on the evolutionary track of low-to-intermediate mass companions that started mass transfer onto a neutron star after they left the main sequence (Podsiadlowski et al. 2002), and have increasing periods. This distinguishes them from the black widows, redbacks, and other low-mass X-ray binaries that have binary periods ⩽1 day, began mass transfer on the main sequence, and evolve toward shorter periods. For 1 $M_\odot$ secondaries, these classes are separated by a bifurcation period of ≈18 hr at the onset of mass transfer.

With $M_2 \approx 0.3\,M_\odot$, the companion of PSR J1417–4402 must have already lost most of its initial mass, only a fraction of which, accreting onto the neutron star, is sufficient to spin it up to 2.66 ms. In the models of Podsiadlowski et al. (2002), PSR J1417–4402 is not far from the ends of the tracks that terminate when the binary period is in the range 6–20 days, and the companion is a He white dwarf of 0.2–0.3 $M_\odot$. The neutron stars in these calculations, assumed to begin with 1.4 $M_\odot$, end in the range 1.8–2.2 $M_\odot$. Exactly how far PSR J1417–4402 is along this evolution is difficult to determine, since its companion may or may not be filling its Roche lobe, may or may not be finished accreting onto the neutron star, and may be losing mass mostly through ablation by the pulsar wind, a process that is difficult to model.

4. CONCLUSIONS

We have discovered a 2.66 ms pulsar in orbit around the 5.4 day optical variable discovered by Strader et al. (2015) in the error ellipse of the high-energy gamma-ray source 3FGL J1417.5–4402. The orbital dynamics require that the companion mass is $>0.2\,M_\odot$. The presence of radio pulsations suggests that the neutron star is not currently accreting (see Section 3.2). The pulsar is only detected a fraction of the time it is observed (although few observations exist at orbital phases $0.65 < \phi_b < 0.9$; Figure 2), and is likely eclipsed for more than half the orbit by outflowing material from the companion; this has so far prevented us from obtaining a phase-connected timing solution.

The DM distance of 1.6 kpc is in conflict with the original estimate of $d = 4.4$ kpc, which was based on the assumption that the companion fills its Roche lobe. This ambiguity then affects most of the remaining interpretation, including the precise evolutionary state of the system, whether it currently has an accretion disk, and the masses, which depend on the modeled inclination angle. The current estimate of $1.77 \leqslant M_1 \leqslant 2.13\,M_\odot$ should really be regarded as an upper

limit. There are several claims of massive neutron stars in redbacks and black widows. Modeling these systems, however, is difficult, especially in the presence of significant heating of the secondary by the pulsar (see, e.g., Romani et al. 2015). So far there is no evidence for heating in the PSR J1417–4402 system, which makes it a good candidate for a precise mass measurement. Further optical observations and modeling of ellipsoidal variations may better determine the inclination angle, and thus the value of M_1, whose uncertainty is currently dominated by the systematic uncertainty on i.

The gamma-ray luminosity of 3FGL J1417.5–4402 is $L_\gamma = 3.7 \times 10^{33}(d/1.6 \text{ kpc})^2 \text{ erg s}^{-1}$ (see Acero et al. 2015), for isotropic emission. At the DM-derived distance this could be accounted for by magnetospheric emission from an MSP with a typical spin-down luminosity $\dot{E} \sim 10\,L_\gamma$. At the larger distance favored by Strader et al. (2015), PSR J1417–4402 would be among the three most luminous MSPs (see Abdo et al. 2013), and might require substantial gamma-ray emission from an intra-binary shock, or a higher than average spin-down luminosity.

A phase-connected timing solution for PSR J1417–4402 will yield its $\dot{E}$ and will allow a search for gamma-ray pulsations. The spin-down luminosity is a fundamental quantity that limits the X-ray and gamma-ray luminosities, and the possible rate of ablation of the companion and of the inner accretion disk if any exists. In addition, a phase-connected solution will place useful constraints on the orbital eccentricity. These quantities should lead to an improved understanding of this unusual system. Finally, the great difficulty we have in detecting the radio pulsar is a reminder that there could be a substantial population of such long-period systems awaiting discovery, which would represent the late phases, until now unobserved, in the formation of typical MSP binaries.

REFERENCES

Abdo, A. A., Ackermann, M., Ajello, M., et al. 2009, Sci, 325, 848
Abdo, A. A., Ajello, M., Allafort, A., et al. 2013, ApJS, 208, 17
Acero, F., Ackermann, M., Ajello, M., et al. 2015, ApJS, 218, 23
Archibald, A. M., Bogdanov, S., Patruno, A., et al. 2015, ApJ, 807, 62
Archibald, A. M., Stairs, I. H., Ransom, S. M., et al. 2009, Sci, 324, 1411
Arons, J., & Tavani, M. 1993, ApJ, 403, 249
Atwood, W. B., Abdo, A. A., Ackermann, M., et al. 2009, ApJ, 697, 1071
Benvenuto, O. G., De Vito, M. A., & Horvath, J. E. 2014, ApJL, 786, L7
Bogdanov, S., Archibald, A. M., Bassa, C., et al. 2015, ApJ, 806, 148
Bogdanov, S., Esposito, P., Crawford, F., III, et al. 2014, ApJ, 781, 6
Bogdanov, S., van den Berg, M., Heinke, C. O., et al. 2010, ApJ, 709, 241
Breeveld, A. A., Landsman, W., Holland, S. T., et al. 2011, in AIP Conf. Ser. 1358, Gamma Ray Bursts 2010, ed. J. E. McEnery, J. L. Racusin, & N. Gehrels (Melville, NY: AIP), 373
Burderi, L., D'Antona, F., & Burgay, M. 2002, ApJ, 574, 325
Burrows, D. N., Hill, J. E., Nousek, J. A., et al. 2005, SSRv, 120, 165
Camilo, F., Kerr, M., Ray, P. S., et al. 2015, ApJ, 810, 85
Chen, H.-L., Chen, X., Tauris, T. M., & Han, Z. 2013, ApJ, 775, 27
Cordes, J. M., & Lazio, T. J. W. 2002, arXiv:astro-ph/0207156
Cordes, J. M., & Lazio, T. J. W. 2003, arXiv:astro-ph/0301598
Cordes, J. M., & Shannon, R. M. 2008, ApJ, 682, 1152
D'Amico, N., Possenti, A., Manchester, R. N., et al. 2001, ApJL, 561, L89
Eggleton, P. P. 1983, ApJ, 268, 368
Frank, J., King, A., & Raine, D. J. 2002, Accretion Power in Astrophysics (Cambridge: Cambridge Univ. Press)
Hill, A. B., Szostek, A., Corbel, S., et al. 2011, MNRAS, 415, 235
Keith, M. J., Jameson, A., van Straten, W., et al. 2010, MNRAS, 409, 619
Linares, M. 2014, ApJ, 795, 72
Manchester, R. N., Hobbs, G., Bailes, M., et al. 2013, PASA, 30, e017
Matthews, A. M., Nice, D. J., Fonseca, E., et al. 2016, ApJ, 818, 92
Orosz, J. A., & van Kerkwijk, M. H. 2003, A&A, 397, 237
Papitto, A., de Martino, D., Belloni, T. M., et al. 2015, MNRAS, 449, L26
Papitto, A., Di Salvo, T., Burderi, L., et al. 2012, MNRAS, 423, 1178
Papitto, A., & Torres, D. F. 2015, ApJ, 807, 33
Pickles, A. J. 1998, PASP, 110, 863
Podsiadlowski, P., Rappaport, S., & Pfahl, E. D. 2002, ApJ, 565, 1107
Ransom, S. M. 2001, PhD thesis, Harvard Univ.
Ray, P. S., Abdo, A. A., Parent, D., et al. 2012, eConf C110509, arXiv:1205.3089
Romani, R. W., Graham, M. L., Filippenko, A. V., & Kerr, M. 2015, ApJL, 809, L10
Roming, P. W. A., Kennedy, T. E., Mason, K. O., et al. 2005, SSRv, 120, 95
Ruderman, M., Shaham, J., & Tavani, M. 1989, ApJ, 336, 507
Sabbi, E., Gratton, R., Ferraro, F. R., et al. 2003, ApJL, 589, L41
Schlafly, E. F., & Finkbeiner, D. P. 2011, ApJ, 737, 103
Stappers, B. W., Archibald, A. M., Hessels, J. W. T., et al. 2014, ApJ, 790, 39
Strader, J., Chomiuk, L., Cheung, C. C., et al. 2015, ApJL, 804, L12
Taylor, J. H., & Cordes, J. M. 1993, ApJ, 411, 674